Electronic Supplementary Material (ESI) for Journal of Materials Chemistry A.

Supporting Information:

Carbon dots-boosted catalytic activity of CaO_2 through tuning visible light conversion

Tingting Cai,[a,b] Wenjing Zheng,[a] Qing Chang,[a] Ning Li,[a] Jinlong Yang,[a,c] Shengliang Hu*[a]

[a] Research Group of New Energy Materials and Devices, North University of China, Taiyuan 030051, P. R. China.

[b] Department of Chemistry and Chemical Engineering, Lvliang University, Lvliang 033000, P.R. China

[c] State Key Laboratory of New Ceramics and Fine Processing, Tsinghua University, Beijing 100084, P. R. China.

1. Materials and methods

1.1 Materials

The coal pitch was smashed and grinded to powder before utilization, and formic acid, H_2O_2 (30%), $CaCl_2 \cdot 2H_2O$, NaOH, sodium acetate, acetic acid, 1, 3, 5-trimethylbenzene (TMB), tetracycline hydrochloride (TC), ethanol, polyethylene glycol 200 (PEG200), 1,4-dicarboxybenzene (TA), ethylenediaminetetraacetic acid disodium salt (EDTA-2Na), vitamin C (VC), isopropanol (IPA) was used as received. The deionized water was used in the preparation of the solution.

1.2 Preparation of CDs

The preparation strategy of CDs was as mentioned in our previous work[1]. 200 mg coal pitch powder was mixed with 30 mL formic acid and 3 mL H_2O_2 (30 wt.%) in the beaker and stirred for 18 h without any external heating. Then the precipitate was separated with the supernatant through the centrifugation of 10000 rpm, and the supernatant was put into the rotary evaporator to get the solid precipitate. Then the precipitate was washed with ethanol and the turbid liquid was dialyzed in water for 2 days. After vacuum drying at 60 °C for 3 h, the dark brown CDs powder was collected.

1.3 Preparation of CaO_2 and CaO_2/CDs

The preparation of CaO_2 was based on a previous report[2] with a slight modification. Thus, 1 mL of 0.1 g/mL $CaCl_2$ solution and 1 mL of 1 mol/L ammonia solution were added to a stirred solution of PEG200 (40 mL) respectively. Then 0.5 mL of 30% H_2O_2 was added dropwise to the solution. After 30 min of stirring, the pH value was

slowly increased to 11.5 by dropwise addition of 1 mol/L NaOH. After stirring for another 30 min, the precipitate was washed with water, ethanol and finally preserved in ethanol. The composite of CaO_2/CDs was prepared by adding CDs to the solution in the first step. Accordingly, the stirring time extended to 3 h (including ultrasonic dispersion of CDs for 10 min). The CDs were prepared from the low-cost coal pitch, as described in our previous report[1]. The colors of these two samples are light yellow and brown respectively, as shown in Figure S2. The optimal conditions were selected through the experiments shown in Figure S3.

1.4 Catalytic oxidation of TMB and TC test

Typically, 10 mL pH 4 NaAc-HAc buffer and 200 μL 30 $mM \cdot L^{-1}$ TMB were mixed, and 2 mg of the sample powder was put into the solution, then the whole system was reacted under stirring of 300 $r \cdot min^{-1}$. The illumination with an energy density of 100 $mW \cdot cm^{-2}$ was provided with the Xenon lamp. Meanwhile, the visible light was obtained with the same lamp with an optical filter of cut-420 nm. After a certain period, the solution was collected and the absorbance was tested with the UV-vis spectrometer.

In the TC degradation experiment, 50 $mg \cdot L^{-1}$ TC fresh solution was prepared before the experiment, and 15 mL was collected each time to mix with 2 mg of CaO_2 or CaO_2/CDs sample to react under the simulated sunlight. The pH of the solution was measured to be around 11. The absorbance of the solution was monitored by taking aliquots at regular intervals.

1.5 H_2O_2 releasing experiment

Firstly, 20 mg samples are added into 60 mL 0.01M buffer solution with magnetic stirring. The illumination and pH are adjusted according to the requirement. After a certain time (30 s, 1 min, 2 min, 5 min, 10 min, 20 min, 30 min), 2mL liquid was absorbed by the syringe and centrifuge with 600 r/min in a centrifuge tube for 2 min. Then 1mL clear liquid was extracted and filtered through the 0.44 μm filter membrane to be added into 2 mL titanium reagent in the cuvette. The titanium reagent was prepared with potassium titanium (IV) oxalate ($K_2TiO(C_2O_4)\cdot 2H_2O$) and sulfuric acid, thus 550 mg $K_2TiO(C_2O_4)\cdot 2H_2O$ was put into the diluted sulfuric acid solution (12.5 mL concentrated sulfuric acid and 487.5 mL deionized water). Then the mixture was put into the UV-vis spectrometer to test and record the absorbance value. After all the data was collected, the absorbance-concentration relationship curve was fitted to the linear equation and then be used to calculate the concentration of the released H_2O_2.

1.6 Active free radical detection

The generation of ·OH could be identified with TA due to the fluorescence properties of 2-hydroxyterephthalic acid (TAOH)[3, 4], which is the combined product of TA and ·OH. Therefore, TA was chosen to measure the generation of ·OH in the water system with CaO_2 and CaO_2/CDs. 5 mg CaO_2 or CaO_2/CDs powder was added into 20 mL TA solution, after lighting for 10 min, 3 mL solution was extracted and centrifuged, the clear liquid was put into the cuvette to measure the PL peak with a fluorescence spectrophotometer. When stimulate with the light of 315 nm, a fluorescence peak at 425 nm appeared, and the data was recorded.

At the same time, NBT[4] was used as the marker of $\cdot O_2^-$. Since the reduction

product diformazan has low solubility in water, the precipitate was collected and redissolved in ethanol with ultrasound to facilitate the dissolution. The blue liquid then was collected to measure the absorbance value to speculate the $\cdot O_2$ amount. It's worth noting that the weak solubility of diformazan in water limited the detection through the UV-vis spectrophotometer. The bluish-violet precipitate needs to be collected and redissolved in an organic solvent, such as DMSO and ethanol, before the absorbance measurement.

1.7 Experiment of reaction dynamics

The reaction dynamics was then studied in a series of TMB solutions with a range of concentration. The absorbance displayed a linear increase in each concentration (Figure S6) and the value of the slop rises gradually. The absorbance data should be converted to TMB-ox concentration according to Lambert beer's law (1) when calculating the velocity.

$$A = \varepsilon \times b \times C \tag{S1}$$

where A is absorbance which can be measured; ε is the molar extinction coefficient of TMB-ox, (ε=39000 $M^{-1}cm^{-15}$); b is the path length of light (b=1 cm).

Then the reaction rates were fitted by the Michaelis-Menten equation:

$$v = V_{max} \times \frac{[S]}{[S] + K_m} \tag{S2}$$

where V_{max} is the maximal reaction velocity; K_m is the Michaelis constant; $[S]$ is the concentration of reaction substrate.

Therein, K_m is a key parameter that indicates the enzyme affinity for a substrate. The lower K_m value means the higher affinity of catalysts to the substrates. V_{max} refers

to the reaction rate when the substrate concentration is saturated.

1.8 Monochromatic light experiment

The monochromatic light was achieved by changing the optical filters of different wavelengths, including 450, 500, 550, 600, 650, 700 nm. Then the photocatalysis to TC was carried out under monochromatic light. To maintain the identical intensity and the light intensity of 60 mW/cm^2 was chosen.

1.9 Sacrificial agent experiment

In the same system with the TMB catalysis experiment, sacrificial agents (2 mg EDTA-2Na, 2 mg VC,1 mL IPA) were used to specially target at the h^+, $\cdot O_2$ and $\cdot OH$ and put into the system before the catalytic reaction. The absorbance of the solution was monitored after the reaction of 10 min.

1.10 Electrochemical measurement

As an electrochemical method[6], the Mott-Schottky curve was adopted to estimate the conduction band (CB) due to the relationship between the flat band and CB. CaO_2/CDs and CDs all show positive slope, which indicates the n-type of the semiconductor, and the conduction band of them both locate in -0.44 V vs. NHE.

The electrochemical measurement was conducted in the solution system of 0.1 M Na_2SO_4 with the three electrodes unit. The working electrode, counter electrode, and reference electrode were the sample-coated ITO glass, the Ag/AgCl standard electrode, and the Pt plate, respectively. The electrochemical data was tested and recorded by the SP-200 Bio-logic electrochemical workstation.

Mott-Schottky (MS) curves were measured in the Na_2SO_4 solution and four frequencies were chosen simultaneously to obtain the flat band potential of the samples**.** Their plots show a negative slope, which is typical for n-type semiconductor[7]. According to the relation of conduction band potential(E_c) and the flat band potential(E_{fb})[8, 9],

$$E_c = E_{fb} - kT \ln \frac{N_D}{N_C} \tag{S3}$$

Therein, k presents the Boltzmann constant, T stands for the temperature. N_D and N_C refer to the donor impurity concentration and the effective conduction band state density. The second term depends mainly on the doping concentration of the semiconductor, and to the heavily-doped n-type semiconductor, it approaches 0 that can be neglected. Therefore, the equation can be written as $E_c \approx E_{fb}$ [10],

$$N_d = \frac{2}{e_0 \varepsilon \varepsilon_0} \left| \frac{dC^{-2}}{dV} \right|^{-1} \tag{S4}$$

in which e_0 refers to the electron charge, ε and ε_0 is the dielectric constant and vacuum permittivity, respectively.

1.11 The Tauc Plot measure

The bandgap of CaO_2 was calculated from the Tauc plot[10, 11] based on the UV-Vis-DRS. The bandgap E_g was calculated through the formula as follows[10, 11],

$$(\alpha h\nu)^{1/n} = A(h\nu - E_g) \tag{S5}$$

in which α is the absorbancy index, h is the Planck constant, ν is the frequency of the incident light, A is constant, Eg represents the bandgap. Especially, n depend on the semiconductor type of the sample, it is 1/2 with direct band-gap semiconductor, and 2

with indirect band-gap semiconductor.

It should be noted that since the photocatalysis was conducted under visible light, the effective bandgap of CaO_2 could be 2.20 eV, which corresponds to the absorption edge at 400-550 nm. Actually, the result can be well accepted considering the photocatalytic effect in Figure 2a.

1.12 The comparison experiment between the in situ generated H_2O_2 from CaO_2 and the externally added H_2O_2

The amount of CaO_2 and the corresponding amount of H_2O_2 was calculated according to the stoichiometric ratio of CaO_2 : H_2O_2 =1:1 with the assumption that CaO_2 can totally convert to H_2O_2. Then the oxidation comparison to catalyze TMB was conducted in the pH 4.0 NaAc-HAc buffer solution with the 100 mW/cm^2 illumination of visible light.

1.13 Cyclic experiment

The reusability experiment was conducted in the alkaline condition to TC. The experiment operation was the same with that in Section 1.4. The difference is that the amount was enlarged considering the loss of powder in the recollection process. Correspondingly, the volume of TC was determined by the amount of catalyst. Therefore, the concentration of catalyst and TC keep the same with that in the general process. After the first test, the catalyst was collected and washed by DI water for 2 times, then the dried powder was collected and weighed to carry on the catalytic experiment for the second time.

1.14 Photocurrent test experiment

The photocurrent test was conducted in the three-electrodes device with 0.1 M $NaSO_4$ as the electrolyte. The working electrode, counter electrode, and reference electrode were the sample-coated ITO glass, the Ag/AgCl standard electrode, and the Pt plate, respectively. The system was put in a dark box and Xenon light was placed out of the box and the light can shine into it through the hole. In the experiment, the dark could be achieved with the hole be blocked. The I-t curves were tested and recorded by the SP-200 Bio-logic electrochemical workstation.

2. Characterization

The samples were characterized by X-ray diffraction (XRD, Rigaku Ultima IV using Cu Ka target), X-ray photoelectron spectroscopy (XPS, Thermo Scientific K-Alpha), scanning electron microscopy (SEM, TESCAN MIRA LMS), transmission electron microscopy (TEM, FEI Tecnai G2 F20), Fourier Transform Infrared Spectrometer (FTIR, Thermo Nicolet iS20), electrochemical workstation (SP-200), diffuse reflectance spectrum (Shimadzu UV-2550), fluorescence spectrophotometer (F-280 Tianjin Gangdong SCI.&TECH.) and fluorescence lifetime spectrometer (Quantaurus-Tau, C11367-32). The absorption spectra were measured on a Shimadzu UV-2550 UV–vis spectrometer.

3. Supporting results

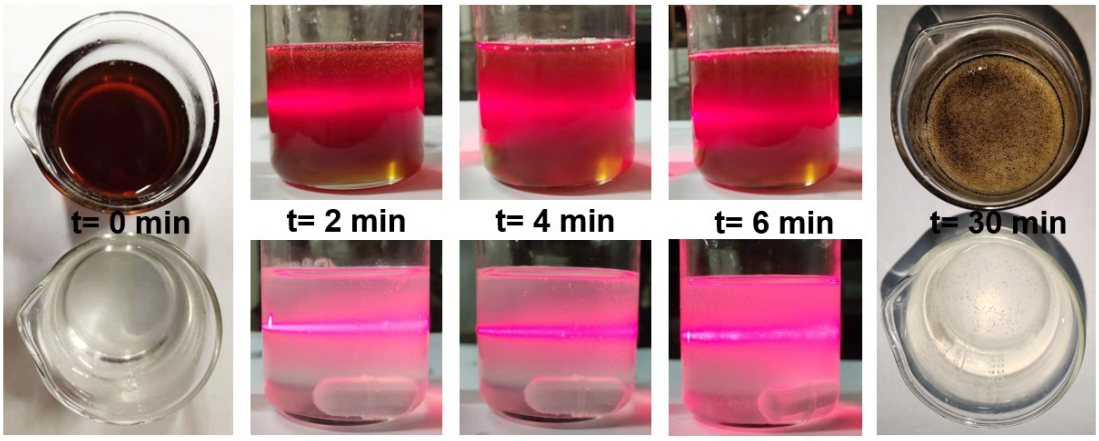

Figure S1. The photos taken at different moment during the synthesize process of CaO_2/CDs and CaO_2. (Above: CaO_2/CDs, Below: CaO_2)

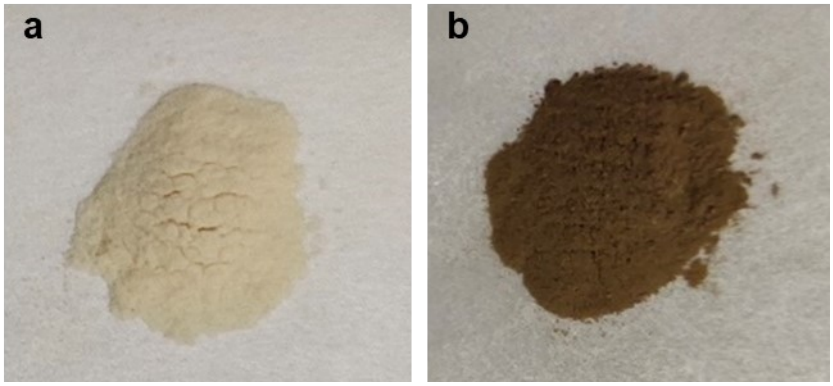

Figure S2. The prepared CaO_2 (a) and CaO_2/CDs (b) powders after desiccation.

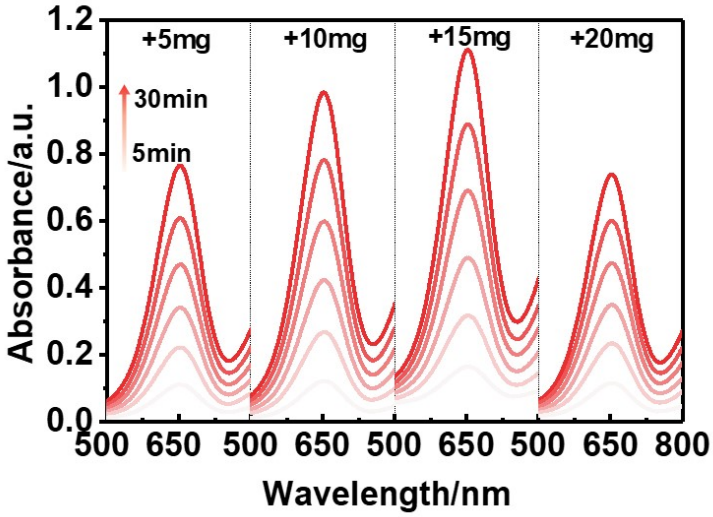

Figure S3. The catalytic activities of CaO_2/CDs with different addition amounts of CDs

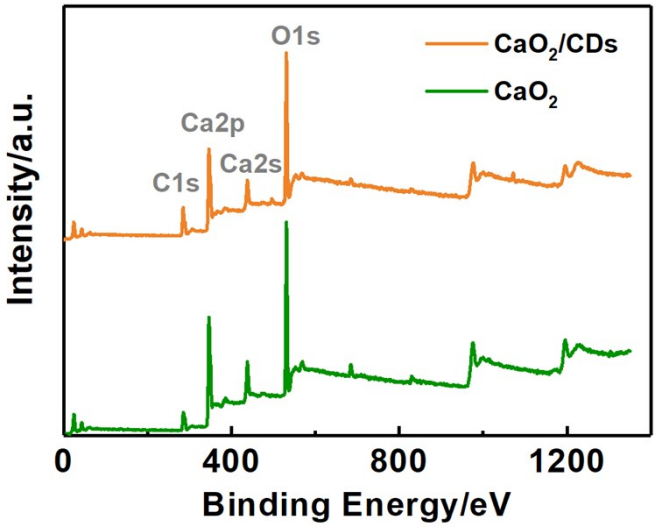

Figure S4. The XPS survey curve of CaO_2 and CaO_2/CDs.

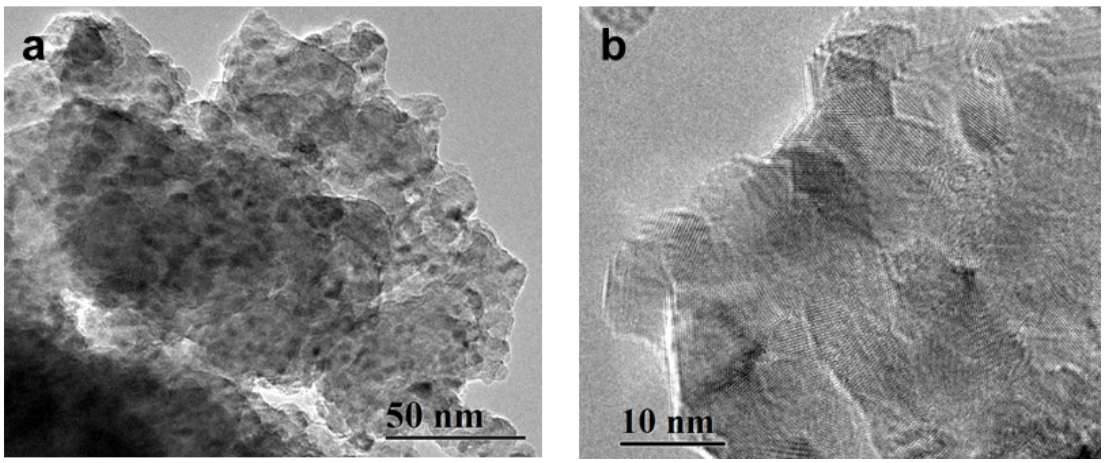

Figure S5. The TEM image of CaO_2 with (a) low-resolution and (b) high-resolution.

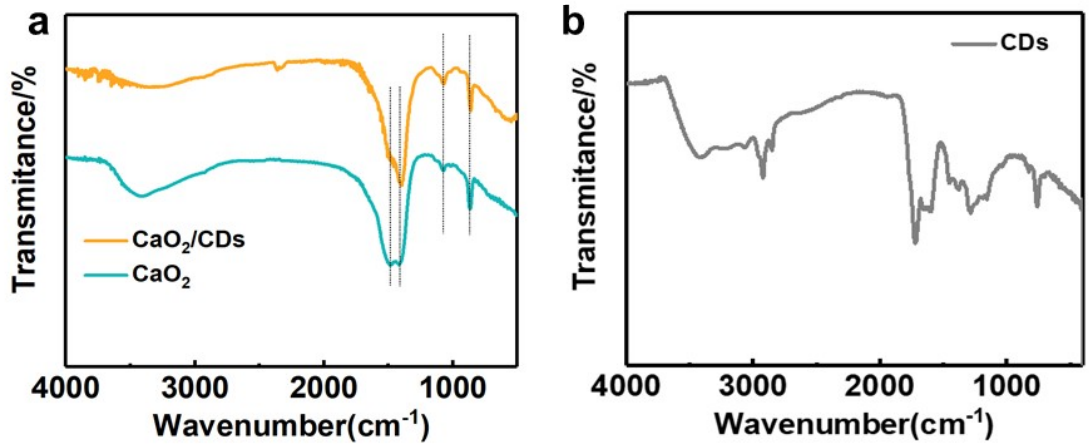

Figure S6. The FTIR curves of (a) CaO_2 and CaO_2/CDs, (b) CDs.

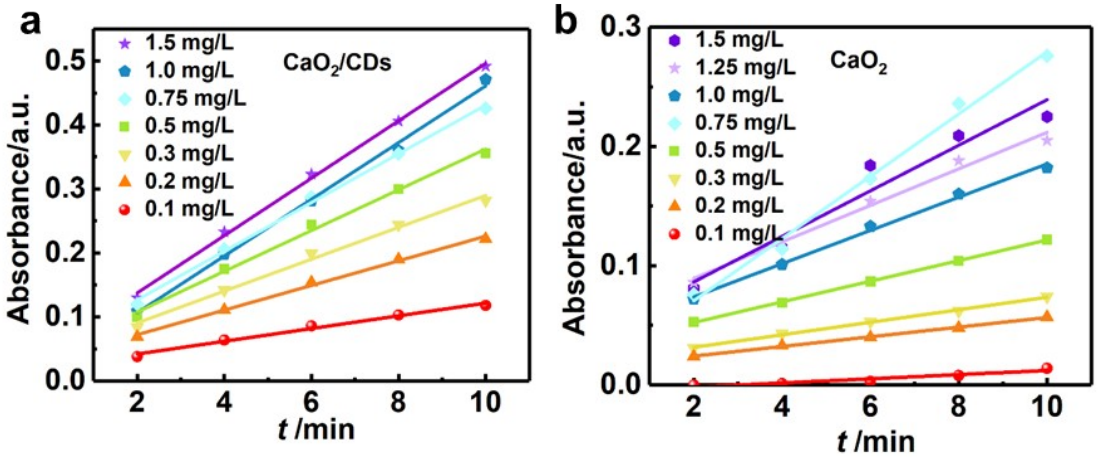

Figure S7. The absorbance of TMB-ox with the different amounts of (a) CaO_2/CDs and (b) CaO_2

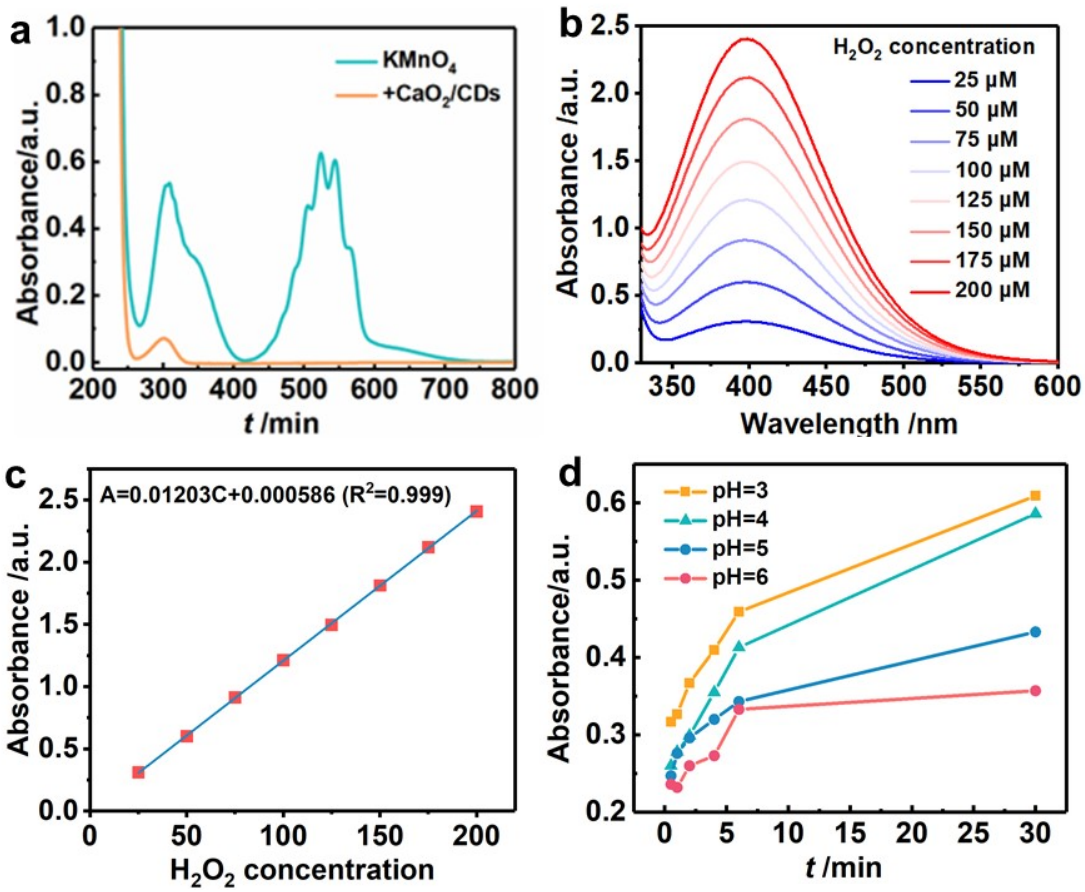

Figure S8. (a) The absorbance of $KMnO_4$ with and without the addition of CaO_2/CDs. (b) The H_2O_2 releasing rate in the solution with different pH. (c) The absorbance curve of titanium reagent with different concentrations of H_2O_2. (d) The linear relation of the absorbance peak at 398 nm and the concentration of H_2O_2.

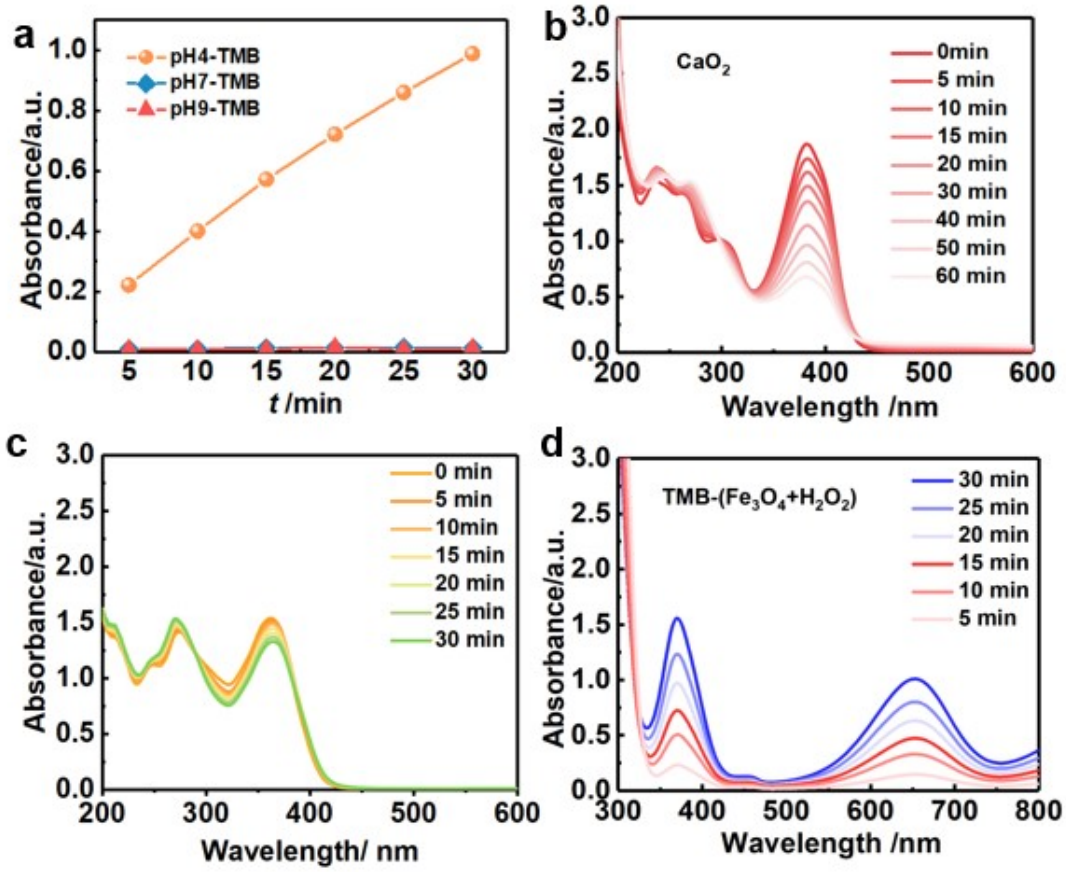

Figure S9. (a) The photocatalytic performance of CaO_2/CDs to TMB at different pH conditions. (b)The absorbance curve of the TC oxidation to time with the addition of CaO_2. (c) The self-photooxidation of TC alone. (d) The catalytic performance of Fe_3O_4 and H_2O_2 to TMB.

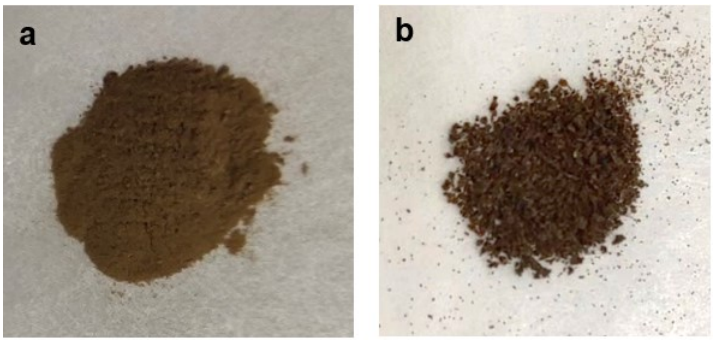

Figure S10. The powder before (a) and after (b) photocatalytic reaction

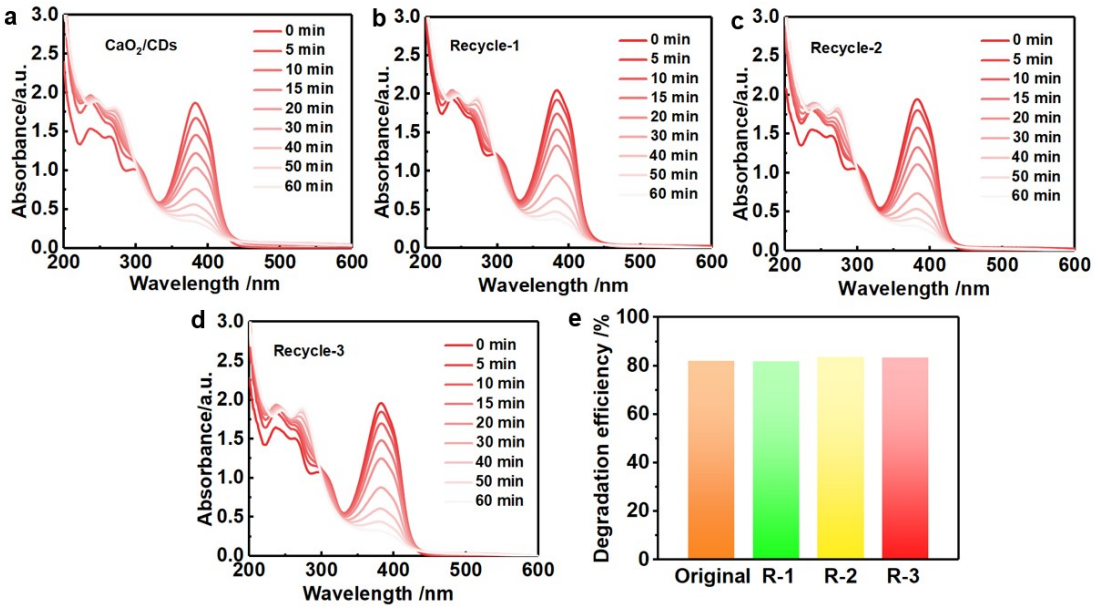

Figure S11. The recycling experiments of CaO_2/CDs to TC degradation: The degradation performance of (a) the first time, (b) the first recycle, (c) the second recycle, (d) the third recycle. (e) The comparison of the degradation efficiency in the recycling experiment.

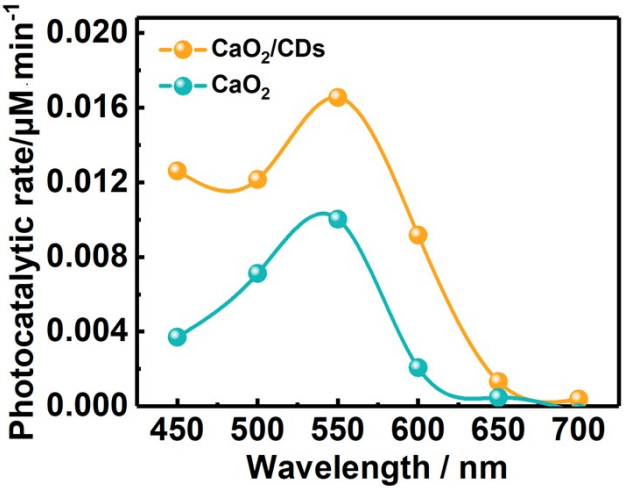

Figure S12. The monochromatic photocatalytic performance of CaO_2/CDs and CaO_2 to TC.

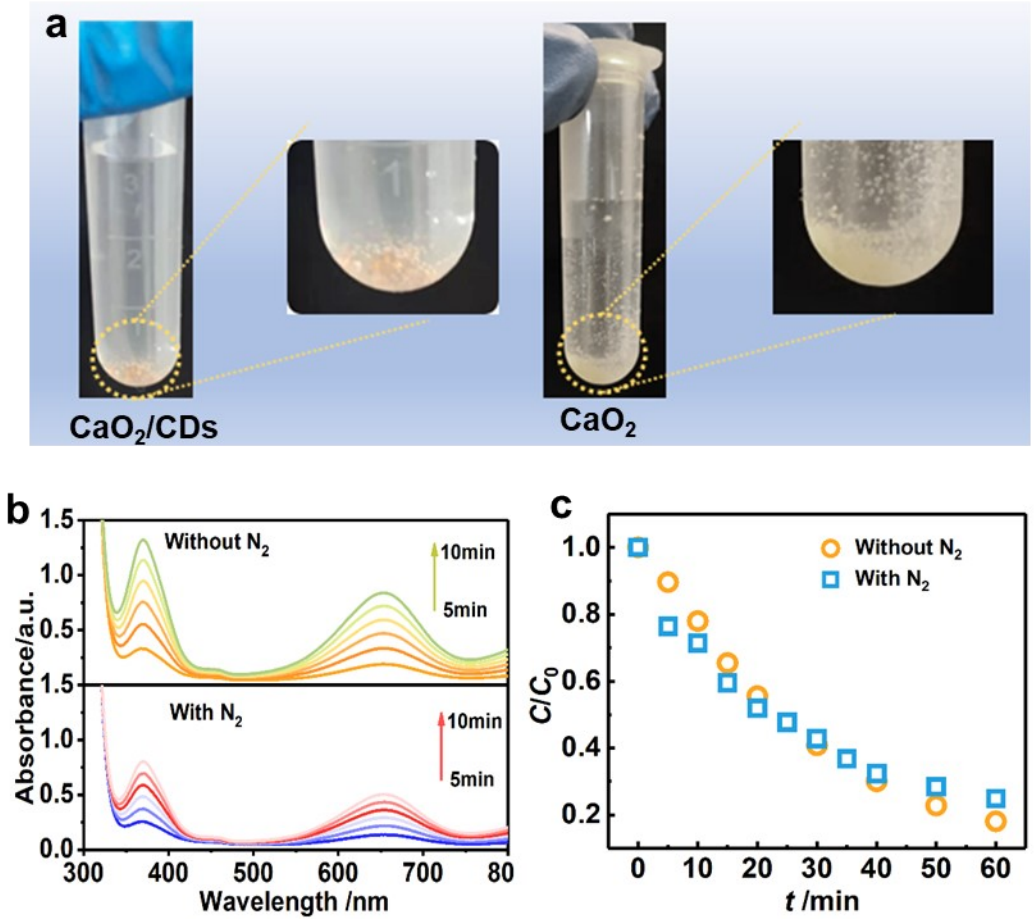

Figure S13. (a) The bubbles appear when CaO_2/CDs and CaO_2 are put into water. (b) The absorbance of TMB-ox at 654 nm with and without N_2 bubbles. (c) The change of the reacted ratio of TC to time with and without N_2 bubbles.

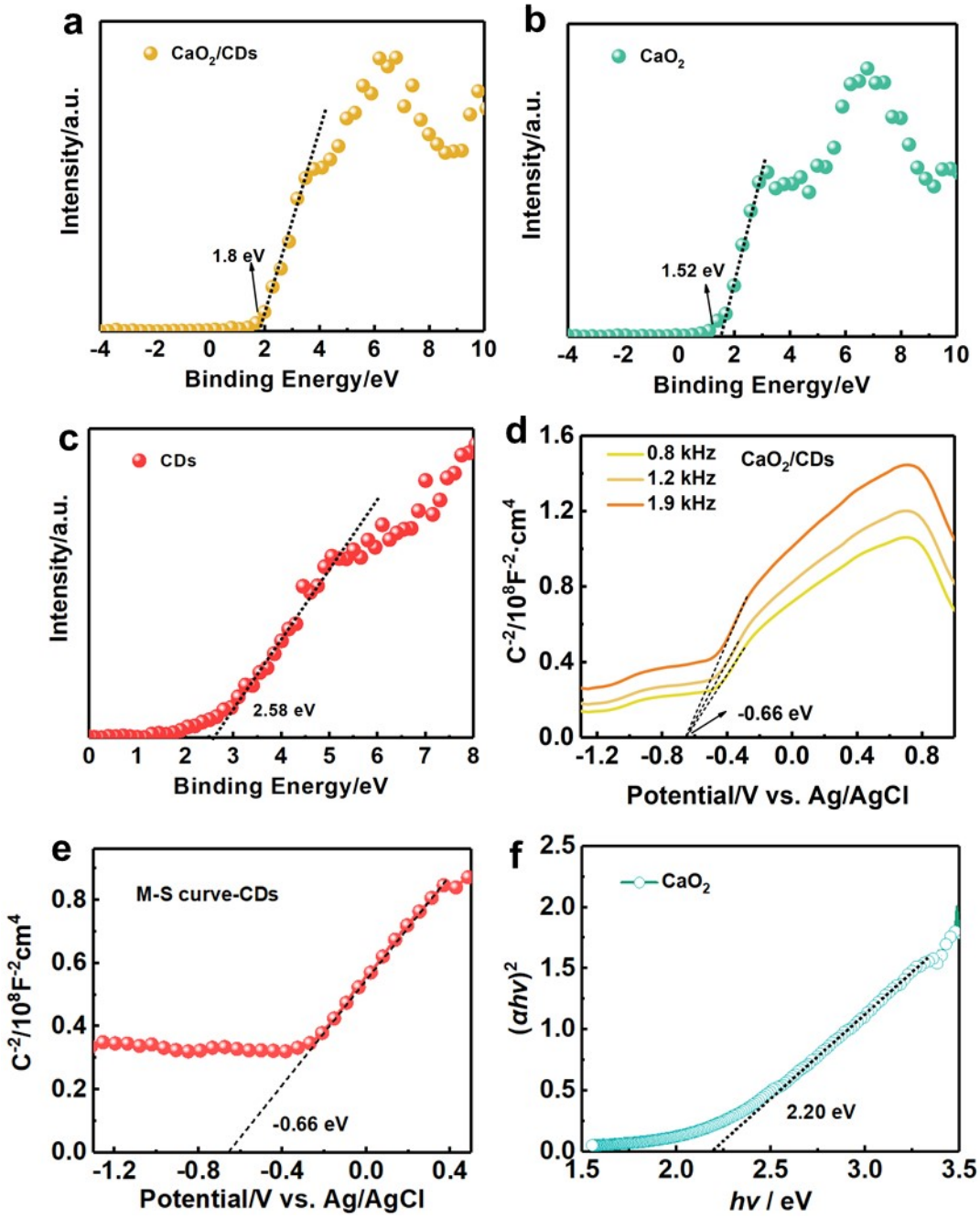

Figure S14. The bandgap analysis of CaO_2/CDs, CaO_2, and CDs. The XPS valence band spectrum of (a) CaO_2/CDs (b) CaO_2 and (c) CDs. MS (Mott–Schottky) plot of (d) CaO_2/CDs and (e) CDs. (f) The Tauc-plot analysis of CaO_2 is based on the UV-vis DRS data.

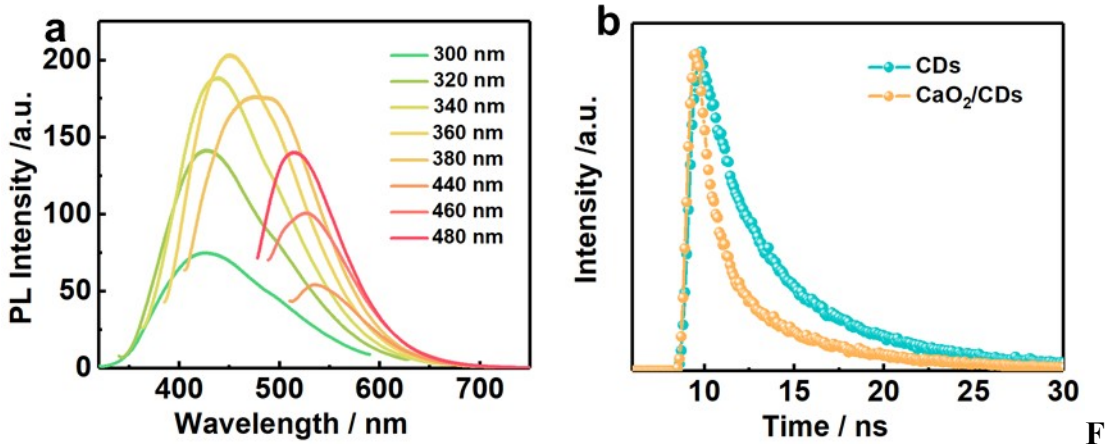

igure S15. (a) The PL performance of CDs with a range of excitation lights. (b) The fluorescence lifetime of CDs and CaO_2/CDs.

Table S1. The element distribution figure and the corresponding data of CaO_2/CDs.

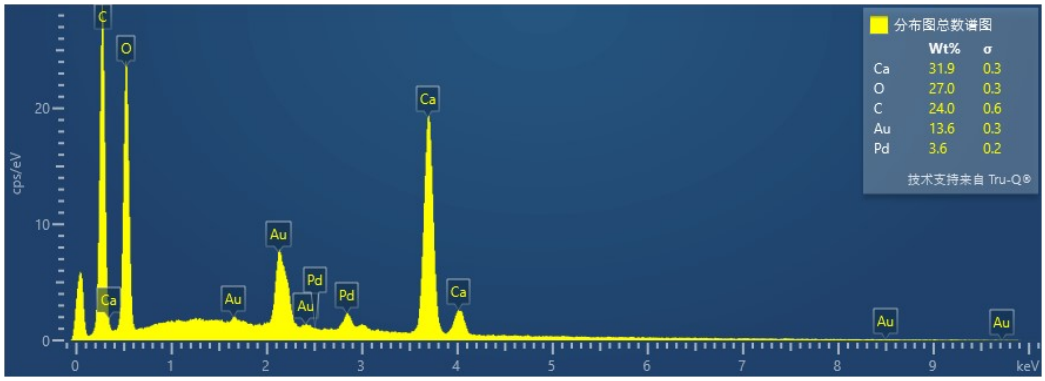

element	Ca	O	C
wt%	31.91	26.95	23.97

Note: The gold (Au) and palladium (Pd) peaks are due to the gold spraying treatment.

References

1. X. Meng, Q. Chang, C. Xue, J. Yang and S. Hu, *Chem. Commun.*, 2017, **53**, 3074-3077.
2. L. H. Liu, Y. H. Zhang, W. X. Qiu, L. Zhang, F. Gao, B. Li, L. Xu, J. X. Fan, Z. H. Li and X. Z. Zhang, *Small*, 2017, **13**, 1701621.
3. Q. Chang, X. Han, C. Xue, J. Yang and S. Hu, *Chem. Commun.*, 2017, **53**, 2343-2346.
4. Y. Nosaka and A. Y. Nosaka, *Chem. Rev.*, 2017, **117**, 11302-11336.
5. W. Shi, Q. Wang, Y. Long, Z. Cheng, S. Chen, H. Zheng and Y. Huang, *Chem. Commun.*, 2011, **47**, 6695-6697.
6. J. Yan, T. Wang, G. Wu, W. Dai, N. Guan, L. Li and J. Gong, *Adv. Mater.*, 2015, **27**, 1580-1586.
7. T.-F. Yeh, C.-Y. Teng, S.-J. Chen and H. Teng, *Adv. Mater.*, 2014, **26**, 3297-3303.
8. S. Navalon, A. Dhakshinamoorthy, M. Alvaro and H. Garcia, *Chemsuschem*, 2013, **6**, 562-577.
9. M. Zhao, J. Zhuang, Q. Cheng, W. Hao and Y. Du, *Small*, 2021, **17**, 1903769.
10. Z. Lin, J. Xiao, L. Li, P. Liu, C. Wang and G. Yang, *Advanced Energy Materials*, 2016, **6**, 1501865.
11. T. C. Araújo, H. d. S. Oliveira, J. J. S. Teles, J. D. Fabris, L. C. A. Oliveira and J. P. de Mesquita, *Appl. Catal., B-Environ*, 2016, **182**, 204-212.